http://dx.doi.org/10.5012/bkcs.2013.34.5.1462

Template-Assisted Electrochemical Growth of Hydrous Ruthenium Oxide Nanotubes

Sanghyun Cho,[†] Lichun Liu,[‡,§] Sang-Hoon Yoo,[†] Ho-Young Jang,[†] and Sungho Park[†,‡,*]

[†]*Department of Energy Science and* [‡]*Department of Chemistry, Sungkyunkwan University, Suwon 440-746, Korea*
[*]*E-mail: spark72@skku.edu*
[§]*College of Biological, Chemical Sciences and Engineering, Jiaxing University, Jiaxing 314001, China*
Received January 22, 2013, Accepted February 18, 2013

We demonstrate that ruthenium oxide (RuO_2) nanotubes with controlled dimensions can be synthesized using facile electrochemical means and anodic aluminum oxide (AAO) templates. RuO_2 nanotubes were formed using a cyclic voltammetric deposition technique and an aqueous plating solution composed of $RuCl_3$. Linear sweep voltammetry (LSV) was used to determine the effective electrochemical oxidation potential of Ru^{3+} to RuO_2. The length and wall thickness of RuO_2 nanotubes can be adjusted by varying the range and cycles of the electrochemical cyclic voltammetric potentials. Thick-walled RuO_2 nanotubes were obtained using a wide electrochemical potential range (–0.2~1 V). In contrast, an electrochemical deposition potential range from 0.8 to 1 V produced thin-walled and longer RuO_2 nanotubes in an identical number of cycles. The dependence of wall thickness and length of RuO_2 nanotubes on the range of cyclic voltammetric electrochemical potentials was attributed to the distinct ionic diffusion times. This significantly improves the ratio of surface area to mass of materials synthesized using AAO templates. Furthermore, this study is directive to the controlled synthesis of other metal oxide nanotubes using a similar strategy.

Key Words : Ruthenium oxide, Nanotube, Electrodeposition, Linear sweep voltammetry (LSV), Ionic diffusion

Introduction

Ruthenium dioxide (RuO_2) is a useful compound with extensive applications in various fields such as catalysis, energy storage, and electronics due to its strong oxidizing properties, reversible reduction-oxidation (redox) ability, and quasi-metallic conductivity.[1-3] In many applications, a large surface area to mass ratio is required for enhanced performance. Vertical nanotube arrays are ideal electrodes for most electrochemical devices because of the large surface area provided by the exposed outer and inner walls along with the thin wall thickness. Due to these features, nanotubes meet the requirement of a large ratio of surface area to mass ratio. Synthesizing vertical nanotubes is fundamentally important in nanotube research, and has received intensive attention.[4] Anodic aluminum oxide (AAO) templates are a powerful and commonly-used scaffold for constructing many type of nanostructures based on a bottom-up strategy, such as nanowires,[5-9] nanorods,[10-17] nanotubes,[18-20] and other more uncommon nanostructures.[21-23] The combination of AAO templates with electrochemical techniques has been used to synthesize RuO_2 nanotubes, resulting in RuO_2 nanotubes that can be used as high-performance electrochemical supercapacitor electrodes.[24] However, there have not yet been any studies of the synthetic controllability of RuO_2 nanotubes. Based on our experience synthesize AAO template-assisted nanostructures, we specifically studied methods to control the length and wall thickness of RuO_2 nanotubes using electrochemical strategies, and we propose a possible mechanism to form RuO_2 nanotube in AAO nanochannels.

Experimental

Chemicals. Ruthenium chloride ($RuCl_3 \cdot 3H_2O$) was purchased from KOJIMA. All aqueous solutions were prepared with ultrapure water (Millipore, > 18.2 MΩ). Au plating solution (Orotemp 24 RTU) was purchased from Technic Inc. Anodic aluminum oxide template membranes (AAO, diameter ≈ 13 mm, nanochannel diameter 300 nm, thickness ≈ 60 μm) were purchased from Whatman International, Ltd.

Instruments. We performed all electrochemical experiments on an electrochemistry workstation (Metrohm Autolab, PGSTAT12) with a three-electrode system using Pt mesh as a counter electrode, Ag/AgCl (3 M KCl) as a reference electrode, and glassy carbon as a working electrode. We acquired SEM images using a JEOL JSM-7401F field emission scanning electron microscope (FE-SEM) and TEM images using a JEOL JEM2100F high-resolution transmission electron microscope (HR-TEM). X-ray photoelectron spectroscopic (XPS) spectra were obtained using an ESCA 2000-VG (Microtech) using monochromatic Al Ka (1486.6 eV) irradiation as the photo source at a chamber pressure of 1.0×10^{-10} mbar.

Methods and Conditions. Prior to using the AAO template, gold (Au) nanoparticles were immobilized on the mesh side of the AAO using vacuum filtration to form a conducting layer.[25] Gold was then deposited (1.5 C at –0.95 V, C: coulomb) to fill inter-particle voids in the conducting layer. Electrochemical cyclic voltammetry combined with an aqueous ruthenium chloride ($RuCl_3$, 40 mM) plating solution was used to synthesize RuO_2 nanotube arrays on AAO templates. The starting potential and sweep rate of cyclic

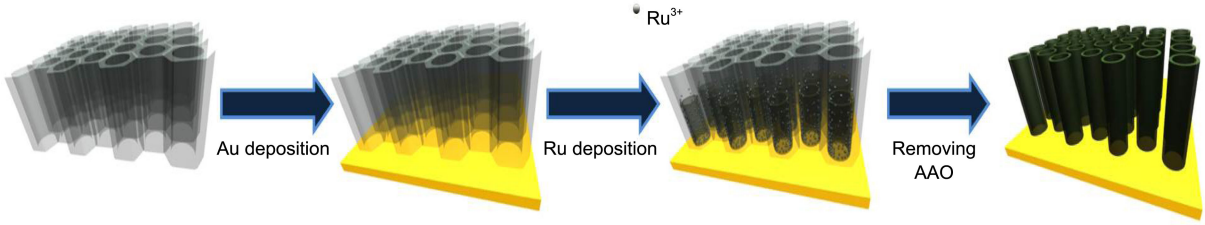

Scheme 1. Schematic illustration of the synthesis procedure of hydrous RuO_2 tubular nanostructure.

voltammetry were 0 V (towards high potential) and 50 mV/s, respectively. The optimal electrodeposition temperature was 50 °C. The RuO_2 nanotube array was obtained by dissolving the AAO template in 3 M NaOH for 20 min at room temperature. After careful rinsing, the RuO_2 nanotube array was further characterized.

Results and Discussion

A Possible Mechanism for RuO_2 Nanotube Formation. The surfaces of most materials are electrically charged when in contact with a polar solution. Charged surfaces are useful for adsorbing species from solution *via* Van der Waals forces, covalent bonding, and electrostatic attraction. The surface of anodic aluminum oxide (*i.e.*, Al_2O_3, alumina) is enriched with hydroxyl groups (-OH) that make it an especially good adsorbent.[26] A number of articles have reported that ions can be adsorbed on the surface of alumina.[27-30] Ru is a typical multivalent noble metal, with oxidation states ranging from −2 to +8. In this work, the most common precursor compound was $RuCl_3$, which has an oxidation state of +3. RuO_2 synthesis is illustrated in Scheme 1. Based on other examples of ionic adsorption on alumina, we propose that trace $RuCl_3$ can be adsorbed on AAO. The ionic adsorption may slightly increase the ion concentration at the wall over that of the solution and at the upper surface of pre-deposited Au (Scheme 2(a)). An applied electrochemical potential drives a chemical change of Ru^{3+} to RuO_2 (the actual chemical form is $RuO_2{\cdot}xH_2O$, but we consistently use RuO_2 here for convenience). The higher Ru^{3+} content at the wall of AAO nanochannels allows RuO_2 to form more rapidly at the wall than any other places. This difference in growth rates gradually results in elevated RuO_2 at the wall. When the height difference in RuO_2 between the wall and any other places reach a critical value, the ionic diffusion aids in the formation of tubular RuO_2 nanostructures because the ions in the nanochannels have a shorter distance to migrate to the nanotube wall than to bottom (Scheme 2(b)).

RuO_2 Characterization. XPS (X-ray Photoelectron Spectroscopy) was used to confirm the presence of RuO_2. XPS core-level spectra from 3d 5/2 and O1s RuO_2 are shown in Figure 1. Spectra from the 3d 3/2 peak were absent because the 3d 3/2 photoelectron signal overlaps with C 1s. The binding energy of 281.38 eV peak was assigned to 3d 5/2 of hydrous RuO_2. The O 1s peak at 530.48 eV can be attributed to hydrous RuO_2. These results confirmed the successful formation of RuO_2 from $RuCl_3$. Similar XPS data have been

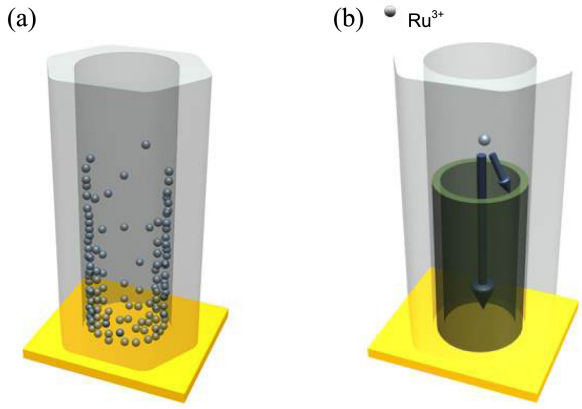

Scheme 2. Schematic illustrations: (a) ionic adsorption on AAO wall, (b) different ionic diffusion rate.

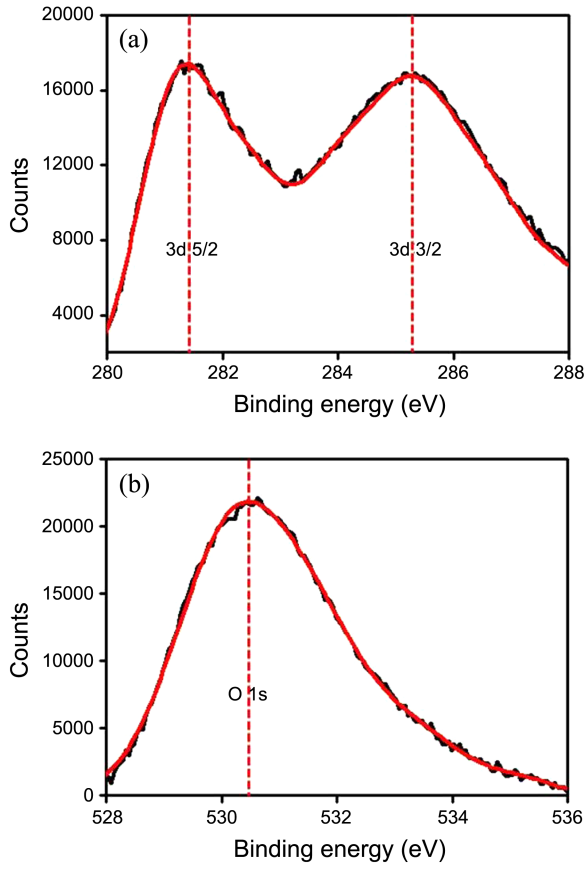

Figure 1. X-Ray Photoelectron spectra of (a) Ru 3d 5/2 and (a) O 1s for electrochemical cyclic voltametric deposition between −0.2 and 1 V (60 cycles).

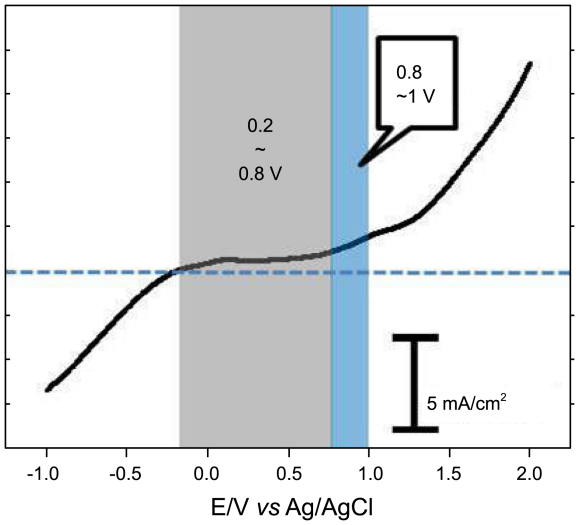

Figure 2. Linear sweep voltammograms (LSV) measured from −1.0 to 2.0 V at a rate of 50 mV/s (gray region: zero-current range, blue region: actual deposition range).

reported previously.[31,32]

Influence of Potential Range. We used linear sweep voltammetry (LSV) to investigate the effective reduction and oxidation potentials for Ru^{3+} (Figure 2). The varied current level seen in Figure 2 indicates the successful reduction and oxidation of Ru^{3+}. Below ~ −0.2 V, there is clearly a rapid drop in cathodic current corresponding to Ru^{3+} reduction. This reduction is not useful for synthesizing RuO_2 nanotubes because anodic current and the oxidation reaction (Ru^{3+} to RuO_2) are required. Between −0.2 V and ~0.8 V (gray region) is almost zero current plateaus during electrodeposition. where there is no redox reaction to effect the formation of RuO_2 nanotube. This zero-current range is critical in CV-based electrochemical deposition. The absence of redox reactions can promote ions to diffuse from high to low concentration regions. Potential over 0.8 V can effectively oxidize Ru^{3+}. Excess positive potential (*e.g.* > 1 V) should be avoided, as it gives rise to a significant oxygen evolution reaction and hinders formation of tubular structure during electrodeposition. The appropriate potential range for Ru^{3+} oxidation was determined to be > 0.8 V by LSV. Direct anodic electrochemical deposition at a constant potential can produce RuO_2. RuO_2 nanotubes have been synthesized using anodic deposition.[24] We demonstrate, however, that cyclic voltammetric (CV) electrochemical deposition is a better technique as it allows for the flexibility to tune the dimensions of RuO_2 nanotube based on distinct ion diffusion times the in plating solution. An ineffective oxidation potential (zero current range, −0.2 ~ 0.8 V in this case) may allow longer ionic diffusion time during deposition.

Influence of Ionic Concentration. The successful formation of RuO_2 nanotubes depends strongly on the $RuCl_3$ concentration in the plating solution at the optimal potential. At low concentrations (*e.g.*, < 40 mM), nanotubes were readily synthesized (Figure 3(a), 20 mM). In SEM images, the nanotube heads had unusual tubular shapes due to significant

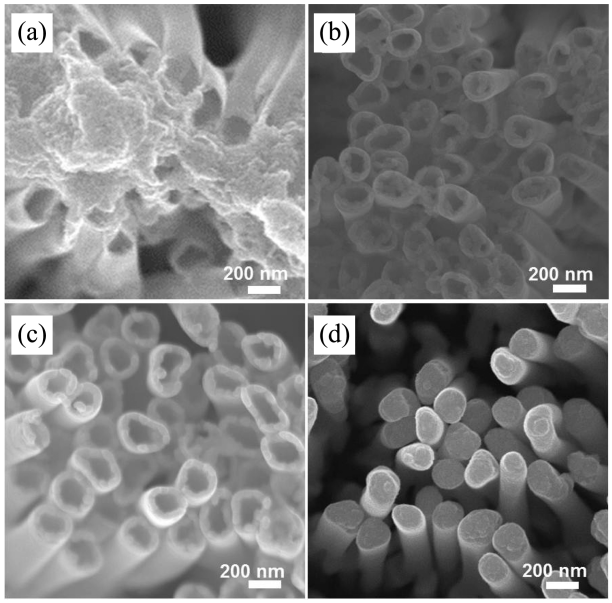

Figure 3. FE-SEM images of RuO_2 nanotubes by controlling different concentration of plating solution with same number of cycles (60 cycles): (a) 20 mM, (b) 40 mM, (c) 60 mM, (d) 80 mM.

inter-tube elastrocapillary coalescence[33,34] during sample drying. At higher $RuCl_3$ concentrations (*e.g.*, 40 mM), tubular structure could be fabricated (Figure 3(b)). At $RuCl_3$ concentrations over 80 mM, however, nanorods were formed (Figure 3(d)) compared with nanotubes from 20 mM (Figure 3(a)), 40 mM (Figure 3(b)) and 60 mM (Figure 3(c)). The nanorods, which are distinct from nanotubes, arise due to the failure to create Ru^{3+} concentration gradient between the wall and elsewhere. In other words, alumina can only adsorb a limited number of ions. When the adsorption reaches

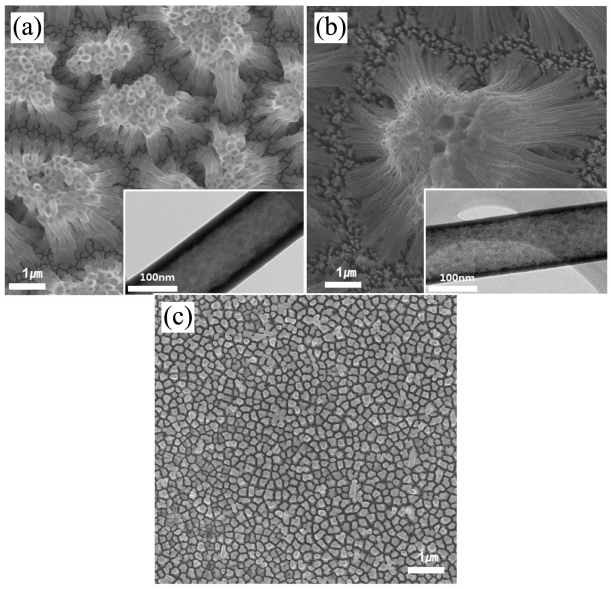

Figure 4. FE-SEM images of RuO_2 nanotubes with different potential range: (a) −0.2 ~ 1 V, (b) 0.8-1 V and (c) −0.2 ~ 0.8 V. The right lower insets show each TEM image.

saturation point, the ion concentration on the walls of the alumina nanochannels will be less than that of the solution. This condition failed to initiate nanotube growth as proposed in Scheme 2, and solid nanorods were formed.

Controlling the Length and Wall Thickness of Nanotubes. During electrochemical processes, a depletion region usually forms near the electrode where the solute concentration differs from the bulk solution. By adjusting the potential range to change the effective ionic diffusion time, we successfully synthesized RuO_2 nanotubes with tunable wall thicknesses. For different potential range (−0.2 ~ 1 V, 0-1 V, 0.4-1 V and 0.8-1 V), nanotube length 4.2(±0.28), 7.4(±0.32), 9.4(±0.71) and 18.3(±0.77) μm, and the wall thicknesses were 35(±3), 23(±2.6), 18(±1.9), and 16(±1.9) nm (Figures 5(a)). In a broad potential range, −0.2 ~ 1 V (−0.2 ~ 0.8 V is a non-redox potential, Figure 4(c): no RuO_2 nanotubes fabricated), the ions diffuse more completely to depletion regions, resulting in thick-walled RuO_2 nanotubes (Figure 4(a)). In contrast, the 0.8-1 V range, which forms a redox potential, forms RuO_2 nanotubes with thin walls (Figure 4(b)). Potential greater than 1 V usually causes failed nanotubes synthesis because intense oxygen evolution affects normal RuO_2 growth underneath substrates. This result suggests that the thickness of RuO_2 nanotube walls can be adjusted by choosing different potential ranges.

We found that, after 20 growth cycles, nanotube length does not increase linearly, but wall thickness does. For 20, 40, 60, and 80 deposition cycles, nanotube lengths were 3.4(±0.25), 4.1(±0.31), 4.5(±0.28), and 4.7(±0.23) μm, and the wall thicknesses were 18(±1.6), 25(±2.3), 33(±1.6), and 41(±2.2) nm (Figures 5(b) and 6), respectively. This non-linear increase in length and linear increase in wall thickness can be attributed to increased RuO_2 resistance along the AAO nanochannel wall, which retards electron transfer from the top of the nanotubes to the bottom conductive electrode. Ions therefore migrate to the more conductive sites, such as the insides of nanotubes, rather than the tops, and are then oxidized. This long ionic migration increases the wall thickness.

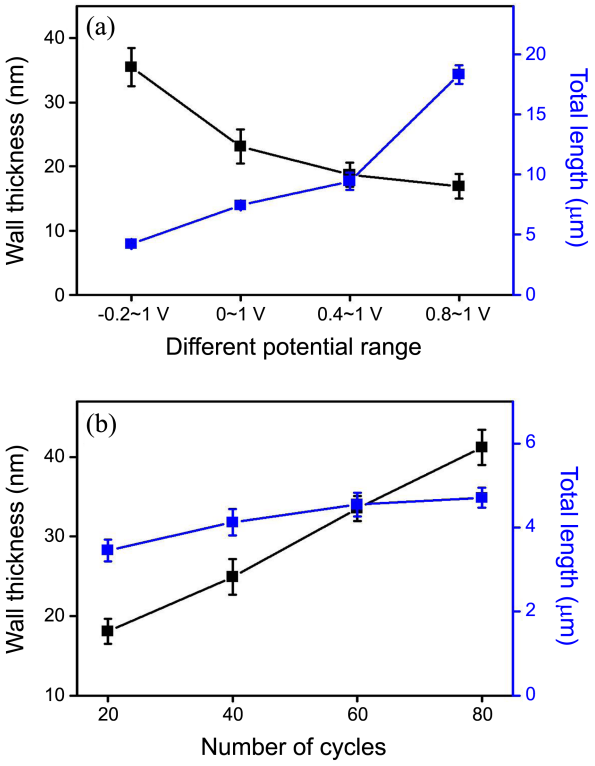

Figure 5. The graphs illustrate the change of wall thickness and total length of RuO_2 nanotubes according to: different potential range (a) and different the number of cycles (b).

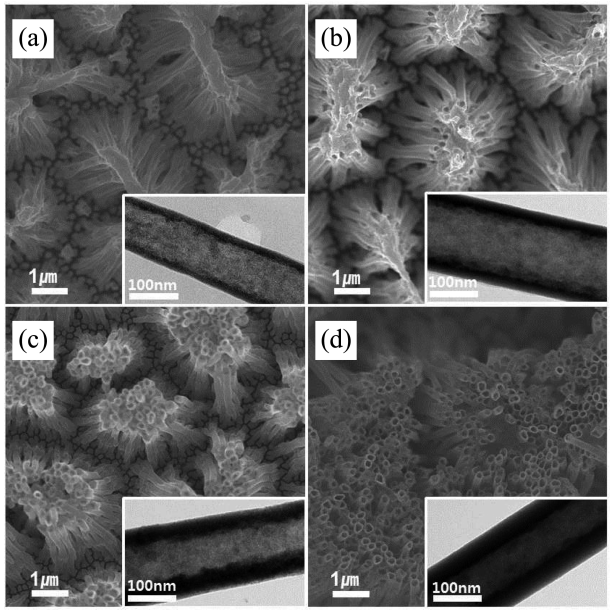

Figure 6. FE-SEM images of RuO_2 nanotubes by controlling the number of cycles: (a) 20 cycles, (b) 40 cycles, (c) 60 cycles, and (d) 80 cycles. The right lower insets show each TEM images.

The concentration of $RuCl_3$ also affects the thickness of RuO_2 nanotube walls, as described in Figure 3. When the $RuCl_3$ concentration is relatively low (*e.g.*, 10 mM), the nanotube walls are too thin maintain their structure, and wall thickness was difficult to evaluate. Theoretically, thinner nanotubes have a large surface area to mass ratio. Practically, nanotubes that are too thin lose surface area due to structural collapse.

Conclusion

In this work, we introduced a method to control the length and wall thickness of RuO_2 nanotubes by electrochemical cyclic voltammetric deposition. We also proposed a possible mechanism for formation of RuO_2 nanotubes in AAO nanochannels. Absence of reduction reaction between −0.2 and 0.8 V could promote ion diffusion rate. Thin-walled RuO_2 nanotubes may provide a large surface area to mass ratio so that materials costs can be reduced. More importantly, this method could allow for guided and controlled synthesis of other tubular nanostructures.

Acknowledgments. This work was supported by the

National Research Foundation of Korea (National Leading Research Lab: 2012R1A2A1A03670370) and by the Human Resources Development program (No. 20124010203270) of the Korea Institute of Energy Technology Evaluation and Planning (KETEP) grant funded by the Korea government Ministry of Knowledge Economy.

References

1. Galizzioli, D.; Tantardini, F.; Trasatti, S. *Journal of Applied Electrochemistry* **1974**, *4*, 57.
2. Over. H. *Chem. Rev.* **2012**, *12*, 3356.
3. Kim, S.; Kim, B.; Jeong, H. G.; Rhee, C. K.; Lim, T. H. *Bull. Korean Chem. Soc.* **2010**, *31*, 3852.
4. Zhang, J.; Ma, J.; Zhang, L. L.; Guo, P.; Jiang, J.; Zhao, X. S. *J. Phys. Chem. C* **2010**, *114*, 13608.
5. Zhang, Q.; Chakraborty, A. K.; Lee, W. I. *Bull. Korean Chem. Soc.* **2009**, *30*, 227.
6. Phok, S.; Rajaputra, S. *Nanotechnology* **2007**, *18*, 475601.
7. Taşaltin, N.; Öztürk, S.; Kilinç, N.; Yüzer, H.; Öztürk, Z. Z. *Nanoscale Res. Lett.* **2010**, 1.
8. Liu, R.; Lee, S. B. *J. Am. Chem. Soc.* **2008**, *130*, 2942.
9. Jung, J. S.; Malkinski, L.; Lim, J. H.; Yu, M.; O'Connor, C. J.; Lee, H. O.; Kim, E. M. *Bull. Korean Chem. Soc.* **2008**, *29*, 758.
10. Kim, S.; Shuford, K. L.; Bok, H.-M.; Kim, S. K.; Park, S. *Nano Lett.* **2008**, *8*, 800.
11. Bok, H. M.; Shuford, K. L.; Kim, S.; Kim, S. K.; Park, S. *Nano Lett.* **2008**, *8*, 2265.
12. Oh, M. K.; Baik, H. J.; Kim, S. K.; Park, S. *J. Mater. Chem.* **2011**, *21*, 19069.
13. Bok, H.-M.; Shuford, K. L.; Jeong, E.; Park, S. *Chem. Comm.* **2010**, *46*, 982.
14. Yoo, S. H.; Park, S. *Adv. Mater.* **2007**, *19*, 1612.
15. Park, S.; Chung, S. W.; Mirkin, C. A. *J. Am. Chem. Soc.* **2004**, *126*, 11772.
16. Kim, S.; Kim, S. K.; Park, S. *J. Am. Chem. Soc.* **2009**, *131*, 8380.
17. Park, S.; Lim, J.-H.; Chung, S.-W.; Mirkin, C. A. *Science* **2004**, *203*, 348.
18. Liu, L.; Yoo, S.-H.; Park, S. *Chem. Mater.* **2010**, *22*, 2681.
19. Liu, L.; Park, S. *Chem. Mater.* **2011**, *23*, 1456.
20. Shin, T.-Y.; Yoo, S.-H.; Park, S. *Chem. Mater.* **2008**, *20*, 5682.
21. Liu, L.; Yoo, S.-H.; Lee, S. A.; Park, S. *Cryst. Growth Des.* **2011**, *11*, 3731.
22. Liu, L.; Yoo, S.-H.; Lee, S. A.; Park, S. *Nano Lett*. **2011**, *11*, 3979.
23. Laocharoensuk, R.; Sattayasamitsathit, S.; Burdick, J.; Kanatharana, P.; Thavarungkul, P.; Wang, J. *ACS Nano* **2007**, *1*, 403.
24. Hu, C.-C.; Chang, K.-H.; Lin, M.-C.; Wu, Y.-T. *Nano Lett.* **2006**, *6*, 2690.
25. Yoo, S.-H.; Liu, L.; Park, S. *J. Colloid. Interf. Sci.* **2009**, *339*, 183.
26. Sprycha, R. *J. Colloid. Interf. Sci.* **1989**, *127*, 1.
27. Sprycha, R. *J. Colloid. Interf. Sci.* **1989**, *127*, 12.
28. Regalbuto, J. R.; Navada, A.; Shadid, S.; Bricker, M. L.; Chen, M. L. *J. Catal.* **1999**, *184*, 335.
29. Agashe, K. B.; Regalbuto, J. R. *J. Colloid. Interf. Sci.* **1997**, *185*, 174.
30. Burke, L. D.; Murphy, O. J.; O'Neill, J. F.; Venkatesan, S. *Journal of the Chemical Society*, Faraday Transactions 1: Physical Chemistry in Condensed Phases. **1977**, *73*, 1659.
31. Mondal, S. K.; Munichandraiah, N. *Journal of Power Sources* **2008**, *175*, 657.
32. Kim, K. S.; Winograd, N. *J. Catal.* **1974**, *35*, 66.
33. Bico, J.; Roman, B.; Moulin, L.; Boudaoud, A. *Nature* **2004**, *432*, 690.
34. Hill, J. J.; Haller, K.; Gelfand, B.; Ziegler, K. J. *ACS Appl. Mater. Inter.* **2010**, *2*, 1992.